GLACIER SURFACE SEGMENTATION USING AIRBORNE LASER SCANNING POINT CLOUD AND INTENSITY DATA

B. Höfle [a,b], T. Geist [c], M. Rutzinger [a,b], N. Pfeifer [d]

[a] Institute of Geography, University of Innsbruck, Innrain 52, 6020 Innsbruck, Austria - (bernhard.hoefle,martin.rutzinger)@uibk.ac.at
[b] alpS - Centre for Natural Hazard Management, Grabenweg 3, 6020 Innsbruck, Austria
[c] FFG - Austrian Research Promotion Agency, Sensengasse 1, 1090 Vienna, Austria - thomas.geist@ffg.at
[d] Institute of Photogrammetry and Remote Sensing, Vienna University of Technology, Gusshausstrasse 27-29, 1040 Vienna, Austria - np@ipf.tuwien.ac.at

KEY WORDS: Airborne Laser scanning, Point cloud, Segmentation, Classification, Intensity, Glaciology

ABSTRACT:

As glaciers are good indicators for the regional climate, most of them presently undergo dramatic changes due to climate change. Remote sensing techniques have been widely used to identify glacier surfaces and quantify their change in time. This paper introduces a new method for glacier surface segmentation using solely Airborne Laser Scanning data and outlines an object-based surface classification approach. The segmentation algorithm utilizes both, spatial (*x,y,z*) and brightness information (*signal intensity*) of the unstructured point cloud. The observation intensity is used to compute a value proportional to the surface property reflectance – the *corrected intensity* – by applying the laser range equation. The target classes *ice*, *firn*, *snow* and *surface irregularities* (mainly crevasses) show a good separability in terms of geometry and reflectance. Region growing is used to divide the point cloud into homogeneous areas. Seed points are selected by variation of corrected intensity in a local neighborhood, i.e. growing starts in regions with lowest variation. Most important features for growing are (i) the local predominant corrected intensity (i.e. the mode) and (ii) the local surface normal. Homogeneity is defined by a maximum deviation of ±5% to the reflectance feature of the segment starting seed point and by a maximum angle of 20° between surface normals of current seed and candidate point. Two-dimensional alpha shapes are used to derive the boundary of each segment. Building and cleaning of segment polygons is performed in the Geographic Information System GRASS. To force spatially near polygons to become neighbors in sense of GIS topology, i.e. share a common boundary, small gaps (<2 m) between polygons are closed. An object-based classification approach is applied to the segments using a rule-based, supervised classification. With the application of the obtained intensity class limits, for ice <49% (of maximum observed reflectance), firn 49-74% and snow ≥74%, the glacier surface classification reaches an overall accuracy of 91%.

1. INTRODUCTION

The cryosphere is a component of the Earth system that presently undergoes dramatic changes. Glaciers and ice sheets as important features of the cryosphere are sensitive to climate fluctuations and their mass balance can be used as an indicator of regional-scale climate change. Next to the quantification of glacier geometry and mass, the qualitative analysis of the glacier surface is important, as for example the identification of the snow line for subsequent parametrisation of glacier mass balance or the classification of different glacier surface facies (e.g. ice, firn, snow). Glaciological research is fundamentally based on field observations, which are rather costly and time-consuming. During the last two decades numerous studies have tested and discussed the possibilities offered by optical and radar remote sensing (summarized e.g. in Rees, 2005; Bamber and Kwok, 2004). Airborne Laser Scanning (ALS) allows for detailed mapping of glacier topography and the quantitative analysis of glacier geometry, such as changes in area and surface elevation, and subsequently mass. Not yet explored is the potential of ALS data for qualitative analysis (e.g. object detection, surface classification).

This paper presents a new method for glacier surface segmentation based on the unstructured point cloud using the full information of ALS data, namely geometry (x,y,z) and signal intensity. The proposed algorithm is fully implemented in a Geographic Information System (GIS). Hence, the GIS vector data model and its topological processing tools can be used. The paper describes in detail the processing and segmentation steps and outlines an object-based classification. While this paper presents an application to glaciers, it shows that a common exploitation of geometry and radiometry provided by laser scanning can be jointly used to successfully segment and classify objects, where neither information source alone would suffice.

1.1 Related work

The last decade has seen increasing interest in the use of ALS for mapping and monitoring glaciers and ice sheets. One motivation was the ability of the technology to map areas of low surface texture (e.g. snow and firn) at high accuracy and resolution. To date, laser scanning for glaciological purposes has been widely and successfully applied in Antarctica and on the Greenland ice sheet (e.g. Abdalati et al., 2002), but only a few attempts have been made to utilize ALS or airborne laser profiling on mountain glaciers (e.g. Kennett and Eiken, 1997; Baltsavias et al., 2001). Geist et al. (2003) and Arnold et al. (2006) give an initial overview on potential applications of ALS in glaciology.

ALS intensity has been utilized in many fields of applications (e.g. road and building detection, strip adjustment, forestry) but only a few studies investigated its value for glaciological research (e.g. Lutz et al., 2003; Hopkinson and Demuth, 2006).

Point cloud segmentation is mostly used for anthropogenic objects/surfaces (e.g. Filin and Pfeifer, 2006; Rabbani et al., 2006). Natural surfaces, such as vegetation or glacier ice, are more likely to have a great variation in terms of geometry and reflectance characteristics. Thus, segmentation of such surfaces into homogeneous regions may be difficult. But separating homogeneous from heterogeneous surfaces already delivers valuable information, as for example the detection of glacier surface irregularities (e.g. crevasses, melt water channels, moulins, debris) surrounded by relatively homogeneous areas.

1.2 Glacier surface characteristics

The paper concentrates on the prevalent glacier surface classes *ice*, *firn*, *snow* and *surface irregularities*. The reflection characteristics of the glacier surface classes in the near-infrared wavelength of the laser scanner used in this study (1064 nm) exhibit a good spectral separability (Wolfe and Zissis, 1993). Due to the decrease of reflectance with age - metamorphosis from new to granular snow and increasing amount of absorbing particles (dirt) - different stages of snow/firn can be distinguished. Typical reflectance values are: glacier ice <0.2, firn 0.5-0.7 and fresh snow >0.7 (Rees, 2005; Hook, 2007). After correcting the laser signal intensity for spherical loss, topographic and atmospheric effects (Section 3.1), it can be used as a value proportional to surface reflectance (Ahokas et al., 2006; Höfle and Pfeifer, 2007). Lutz et al. (2003) and Hopkinson and Demuth (2006) state that the intensity is a good indicator for glacial surfaces (Fig. 1).

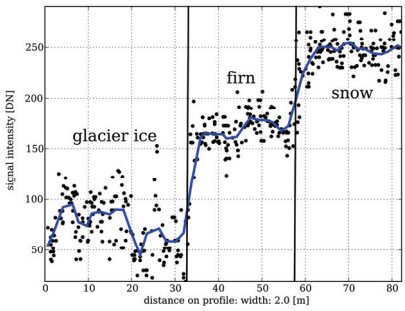

Figure 1. Corrected intensity cross-section along different surfaces: glacier ice, firn and snow. Moving average line clearly shows steps in intensity between the surface classes. Also high variability in intensity of glacier ice areas can be seen

Additionally to the corrected intensity, surface roughness can be used to describe the different classes. In general, terrain variation is increasing with proceeding melting from snow to uncovered glacier ice where irregularities due to glacier dynamics reach the upper surface, and hence are visible for the laser scanner.

2. STUDY AREA AND DATA SETS

2.1 Test site and data acquisition

Hintereisferner (Fig. 2) is a typical valley glacier with a length of approximately 6.5 km along the flow line (determined in 2005). The glacier shows a longitudinal profile with a relatively flat tongue and a steeper accumulation area. For the study described here data from 12 August 2003 is used, when most of the glacier, except the uppermost parts, was free of snow. The ALS flight campaign configurations are summarized in Table 1.

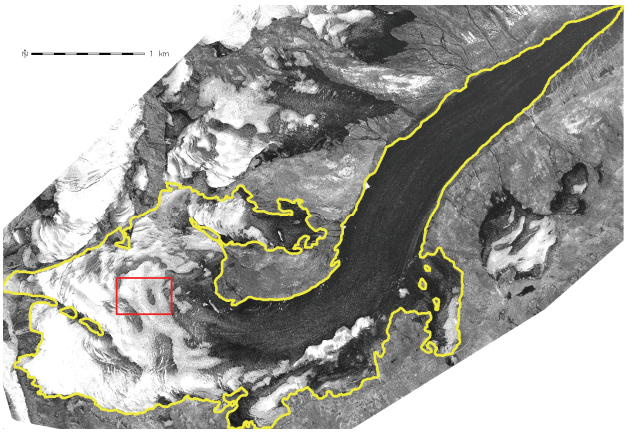

Figure 2. Corrected intensity image of Hintereisferner with glacier borders and rectangular test site

ALS campaign	
date, time	12.08.2003, 6:30–9:21
scanning system	Optech ALTM 2050
laser wavelength	1064 nm
avg. height above ground	1150 m
pulse repetition frequency	50 kHz
scan frequency	30 Hz
scan angle	+/– 20°
swath width	837 m (with 40% overlap)
avg. point density	1.7 points/m^2

Table 1. ALS flight campaign parameters

2.2 Reference data

Traditional aerial images were taken at the same day as the ALS campaign. These images were processed to orthophotos (0.5 m resolution). In order to obtain ground truth for validation, reference data for evaluating the results was created by a glaciologist aware of the local conditions. The classes ice, firn and snow were digitized using the orthophoto and the corrected intensity image. Surface irregularities were identified in the shaded relief of the ALS elevation model.

2.3 Datasets and data management

The ALS point cloud is managed within the LISA (LIdar Surface Analysis) framework (Höfle et al., 2006), which integrates full GIS functionality provided by the Open Source GIS GRASS. The results of the segmentation (segment polygons) are stored in the GRASS vector data model providing topologic geometry storage and attribute data management. For the glacier surface segmentation only single echo points are used. Plane positions, needed for intensity correction, are made available by LISA for each laser shot using linear interpolation of the GPS positions. A test site representing all target classes with 485 m x 318 m extent and 335.104 laser points was selected (Fig. 2).

3. METHODOLOGY

The developed methodology for glacier surface classification is shown in Fig. 3. The major processing steps will be described in detail below.

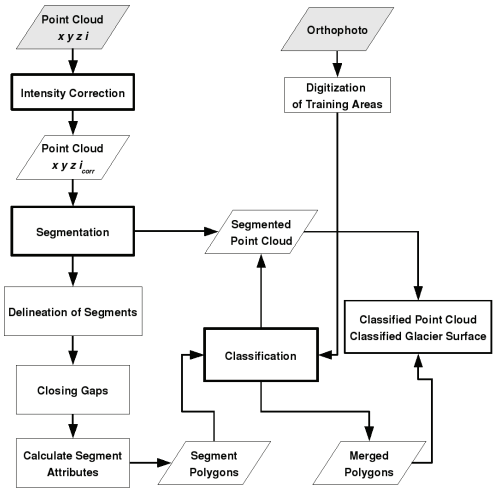

Figure 3. The workflow of glacier surface classification using the original, unstructured ALS point cloud

3.1 Intensity correction

To get a value proportional to surface reflectance, a correction procedure accounting for spherical loss, topographic and atmospheric effects has to be applied. The emitted power is assumed to be constant for the chosen flight campaign because scanner settings, such as pulse repetition frequency, are not changed. The existing data situation allows only for applying a model-driven correction approach (Eq. 1), due to the lack of multiple flying altitudes over homogeneously reflecting areas. Further details concerning intensity correction are described in Ahokas et al. (2006) and Höfle and Pfeifer (2007).

$$\rho \propto I \frac{R^2}{R_S^{\,2}} 10^{2Ra/10000} \frac{1}{\cos \alpha} \quad (1)$$

where ρ = reflectance
I = signal intensity [digital number (DN)]
R = range [m]
R_S = standard/normalizing range [m]
a = atmospheric attenuation coefficient [dB/km]
α = angle of incidence [°]

The intensities are normalized to 1000 m range. Under the assumption of Lambertian scattering characteristics of the surface this value is proportional to surface reflectance and will be called *corrected intensity* in the following. The surface normal is estimated by fitting an orthogonal regression plane to the 30 nearest neighbors and a vertical atmospheric attenuation coefficient of 0.15 dB/km was derived by modeling the atmospheric conditions at time of flight. Fig. 4 shows the evident reduction of disturbance in intensity after correction and Fig. 2 the corrected intensity image of Hintereisferner.

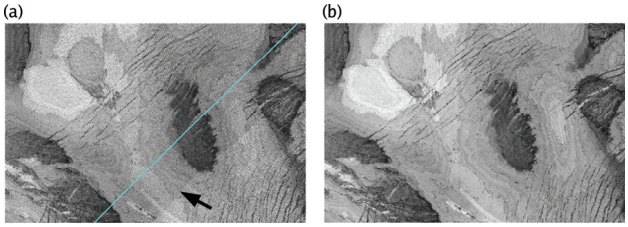

Figure 4. a) image of mean recorded intensity with flight path (cyan); strip offsets can be clearly seen (arrow), b) mean corrected intensity image

3.2 Segmentation

The point cloud is subdivided into homogeneous segments using a geometrical and intensity homogeneity criterion. Segments are defined as spatially connected regions, allowing only smooth terrain transitions (break at step edges, such as crevasses, water channels and glacier borders) and similar intensities. The segmentation steps are (i) point feature calculation, (ii) seed point selection and (iii) region growing.

3.2.1 Feature calculation: For each laser point the features are calculated from its 2D *k* nearest neighbors (kNN). The surface normal is estimated by fitting an orthogonal regression plane. Additionally, the standard deviation (SD) of the orthogonal fitting residuals is used as parameter for surface roughness. A representative corrected intensity value is found in the histogram by choosing the most frequent value (mode) for a given bin size. Hence, the predominant surface is selected and the influence of noise and outliers is reduced. Additionally, the coefficient of variation (c_v) of the corrected intensity is used as parameter for surface homogeneity in the local neighborhood.

3.2.2 Seed point selection: The laser points are sorted by homogeneity (c_v). The lower the variation, the more likely the point lies within a homogeneous area, representing a single surface class, well suited as start point for growing a segment. The seed points could be limited by a certain c_v threshold. Due to the inherent reflectance variation of natural surfaces and to reach an area-wide segmentation, all laser points are accepted as seed points ordered ascending by c_v.

3.2.3 Region growing: The local connectivity of segments is forced by using a small local neighborhood (e.g. *k*=15) and a maximum growing distance, as well as a maximum distance of a neighbor to the current adjusting plane of the segment (either the local surface plane of the starting seed, the current seed or the fitted plane to all current region points). To maintain similarity in terms of smoothness, the angle between the current segment plane and the surface normal of a candidate point is checked. The similarity in terms of reflectance is checked by comparing the current segment corrected intensity (either intensity feature of starting seed, current seed or mean of all current region points) with the corrected intensity feature of the candidate point. The difference must be lower than a defined percentage of the current segment intensity, i.e. for brighter objects higher absolute variation is allowed.

3.3 Delineation of point cloud segments

To be able to use an object-based classification procedure, the delineation (polygonization) of point cloud segments is necessary. The segment boundary line is derived individually for each segment by calculating a 2D basic alpha shape (i.e. based on the Delaunay triangulation of the point set) for a given alpha value (Edelsbrunner and Mücke, 1994; Da, 2006). Small alpha values not necessarily produce a convex shape. If alpha is chosen very large (alpha→∞), the alpha shape represents the convex hull. Before calculating the alpha shapes a minimum segment size threshold (no. of points) is applied, which removes small, isolated points/regions, such as small snow spots or debris. The alpha value has to be chosen such that a connected exterior boundary can be produced. The alpha complex consists of non-ordered boundary line segments. Using GIS tools a clean polygon boundary is built (connect line segments; remove duplicate vertices and small islands; Fig. 5).

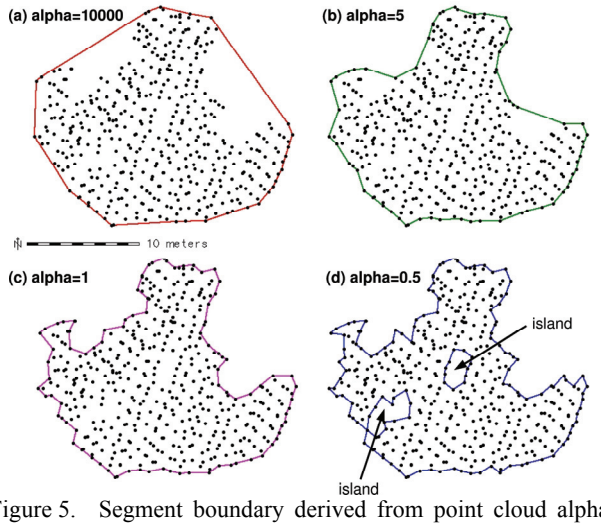

Figure 5. Segment boundary derived from point cloud alpha shape using different alpha values. a) With alpha=10000 the convex hull is reached, d) with small alpha values islands can occur

3.4 Removal of overlaps and closing of gaps between segment polygons

As the segment polygons are derived individually small overlaps and gaps may occur between the single segment polygons. With higher alpha values, more overlapping is necessarily produced. The lower the density of acquired points, the more areas are not covered by a polygon. Cleaning of segment polygons is proceeded as following (Fig. 6):

1. Buffer polygons (define max. gap size) and intersect with gap areas (areas not covered by any polygon).
2. Create Voronoi diagrams of segment boundary vertices. Voronoi polygons get ID of corresponding segment.
3. Intersect gap areas within buffer size with Voronoi diagrams. Assign segment ID to intersection polygons.
4. Merge intersection polygons with segment polygon sharing same ID.
5. Merge overlapping areas (intersections) and very small areas (<2.0 m^2) with adjacent segment sharing longest boundary.

The buffer size should not be too large (e.g. half of estimated gap size) because the segments also grow into the areas not covered by any segment, which are later used to identify surface irregularities. After closing small gaps spatially near polygons share a common boundary line and therefore agree with the definition of neighbor in sense of GIS vector topology.

3.5 Calculate segment attributes

The segment attributes are directly derived from the point cloud (Sect. 3.2.1) but also from the segment polygon. Most important attributes are number of points, descriptive statistical values (e.g. min, mean, max) for elevation, corrected intensity, roughness (SD of plane fitting), as well as polygon area, point density and compactness (perimeter / (2 * sqrt(PI * area)).

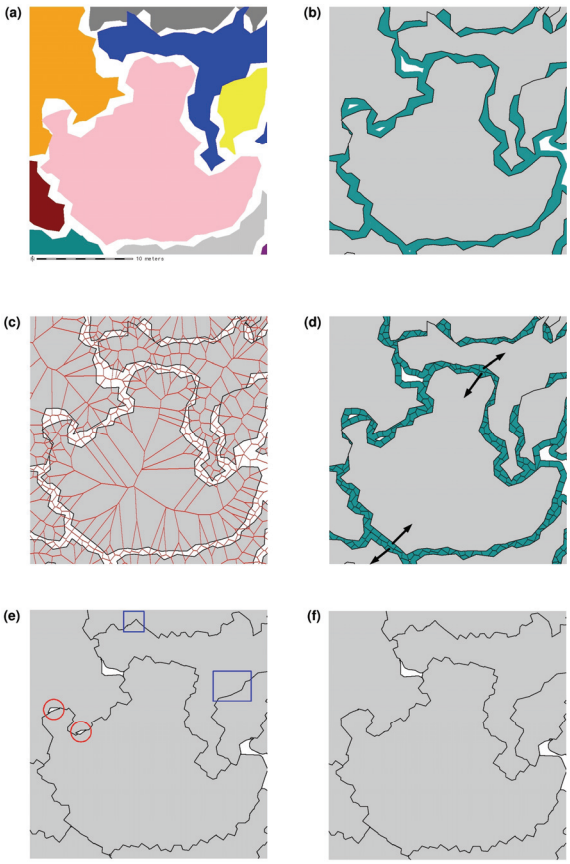

Figure 6. a) segment polygons derived from alpha shapes, b) 1.0 m buffer (green) c) Voronoi diagrams (red lines) of boundary points, d) intersection of Voronoi diagrams with buffer area, e) intersection areas attached to segment polygons; overlaps are already removed (blue squares), small leftover areas to be removed (red circles), f) resulting segment polygons after filling gaps and removing overlaps

3.6 Classification

To show the potential of the proposed segmentation for glacier surface mapping, a simple rule-based classification with manually defined training areas is applied. Training areas are digitized on basis of the orthophoto (Fig. 7b). In a first step the range of corrected intensity values for each target class is derived from the segments spatially selected by the training areas. The second classification feature roughness is preliminary grouped into three classes: low <0.1 m, medium 0.1-0.25 m, and high ≥0.25 m (Kodde et al., 2007). In a second step the segments are labeled according to the classification (e.g. snow with low roughness, ice with medium roughness). Polygons of areas not covered by any segment are derived and labeled as class *surface irregularities*. Using the compactness of the polygon shape the irregularities could be further divided into "longish" (e.g. if high roughness: crevasses, low roughness: superficial stream) and "compact" (e.g. moulins). Using the segment ID the classification can be assigned to the laser points resulting in a classified point cloud.

3.7 Merge of segments - dissolving of common boundaries

Due to the cleaning of the vector topology (e.g. close gaps, remove overlaps) neighboring segments falling into the same class can be easily dissolved along shared boundary lines to

larger polygons. The IDs of the segments are stored and therefore the connection to the segment attributes is kept.

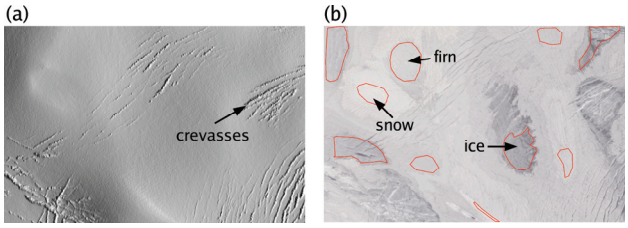

Figure 7. Test site: a) shaded relief b) orthophoto with training areas

4. RESULTS

A fundamental result of the proposed algorithm is the corrected intensity, which can be used to produce undistorted intensity images (Figs. 2 and 4b). Intensity offsets between flight strips and topographic effects have been successfully removed. Using the intensity mode of a given neighborhood for segmentation leads to a removal of outliers and small surface structures (e.g. debris), but also results in a certain classification of the intensity dependent on the chosen bin size of the histogram. A bin size of 5% of the total value range (max. 20 classes) for 50 kNN delivers appropriate values. If the bin size is too small, the mode is not representative anymore. If it is chosen too large, spectral classes are lost. To guarantee defined intensity homogeneity a maximum deviation of ±5% to the intensity of the segment starting seed point is set for growing. To allow smooth terrain transitions but stop growing at step edges, a maximum angle of 20° between the surface normals of current seed and candidate point is specified. The angle criterion is set low enough to get segment boundaries fitting well to the edges of crevasses (Figs. 7 and 8). The alpha shape value for segment delineation should be larger than the double average point spacing else too many islands are produced. An alpha value of 1.5 m was set due to the 0.7 m avg. point spacing of the test site. A larger alpha value would lead to more overlapping segments. Closing gaps between adjacent segment polygons is necessary because the boundaries are individually derived. The double of the buffer around the polygons determines the maximum gap size that is closed. A buffer size of 1.0 m was chosen, and hence gaps of max. 2.0 m are closed but also non-covered areas are shrinked or even fully closed, such as narrow crevasses. Filling gaps and cleaning of polygons is computationally very expensive (a lot of intersection with many polygons). If contextual information is not needed for classification, one could first classify the point cloud, merge the points of adjacent segments of the same class and then derive the boundaries and close gaps. But in comparison to our approach, the question of how to define a clear adjacency of point cloud segments can be more ambiguous.

The classification rules are determined using the manually delineated training areas. The distributions of the three classes partly overlap. The following corrected intensity values (in percentage of maximum observed value in test site) were extracted: ice 38% (11.3% SD), firn 64% (6.7% SD) and snow 85% (6.2% SD). In the ice areas of our test site also small snow and firn spots can be found, which results in a high SD for ice areas. The upper ice class limit is set to class mean+1 SD, whereas for firn and snow a class limit of mean±1.5 SD is used. Hence, the classification rules are: ice <49%, firn 49-74% and snow ≥74%. The roughness feature is not used to identify the surface classes but to independently subdivide the objects into the roughness classes low, medium and high (Sect. 3.6). The areas remaining uncovered even after filling gaps emerge from areas with no laser points or areas with a high variability in intensity or elevation. These areas are summarized as "surface irregularities". Once the segments are classified, the building of larger units by merging neighboring segments is straightforward.

Error assessment was performed using a point wise comparison method. For that purpose the classified point cloud was additionally labeled according to the reference map. The overall classification accuracy turned out to be 90.92%, whereas the spatial accuracy of the object boundaries strongly depends on point density and distribution. The given average point spacing of 0.7 m and closing of gaps <2.0 m fully agree with the state-of-the-art requirements for operational tasks in glacier monitoring, which state a min. horizontal accuracy of ±2 m, in most cases even lower, to be sufficient (Jackson et al., 2001). Ice areas were found to have a good separability but there is a weak transition between firn and snow (Fig. 8), which can be explained by the advanced age of the snow (in August).

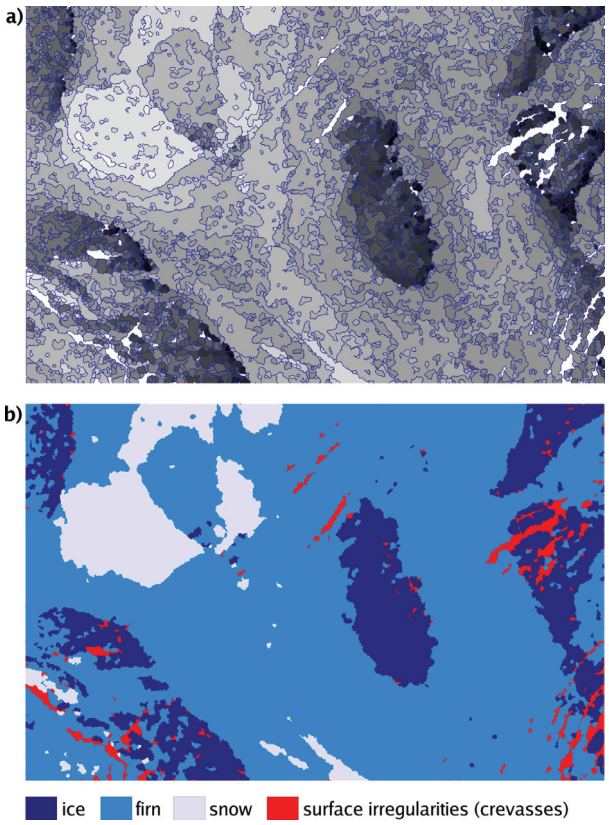

Figure 8. a) Segments colored by mean corrected intensity (black - low intensity, light gray - high intensity, white - unsegmented); b) glacier surface classification

5. CONCLUSIONS

The paper has presented a new workflow for glacier segmentation and classification using spatial and intensity information of the unstructured ALS point cloud. Most ALS sensors already record signal intensity, hence available without additional costs. Homogeneous objects concerning reflectance could be successfully derived. ALS intensity data surpasses the orthophoto in distinguishing between ice and firn (or snow), and in areas with shadows, which are very often in high mountainous areas. The accuracy of the classification is

certainly sufficient for glacier inventory mapping but should be assessed for applications in detailed scales, as for example collect GPS data of distinct objects (e.g. ice and snow spots, crevasses). The segmentation, i.e. the zoning of the glacier into areas with homogeneous surface characteristics, highly reduces data with defined loss of information (homogeneity criteria), and already represents a valuable input for energy balance and melt process models. For the conversion of corrected intensity (DN) to reflectance values defined reflectance targets are needed (Ahokas et al., 2006). The surface classification supports glacier monitoring and facilitates the creation of glacier inventories solely using ALS data. The class "surface irregularities" is important for multitemporal analyses, such as feature tracking of objects for flow velocity estimation or glacier dynamics monitoring (e.g. closing and opening of crevasses). Future work will concentrate on

- applying the methodology to larger areas with more surface classes (e.g. debris, water). Additional classification features have to be selected (e.g. use roughness for surface identification).
- utilization of geometrical and contextual relationships provided by the segment vector topology
- object-based error assessment (spatial and qualitative accuracy) of the classification. Ground truth data has to be collected.
- improving the intensity correction by applying individual reflectance functions for the detected surface classes (e.g. anisotropic reflectance for snow)

REFERENCES

Abdalati, W., Krabill, W., Frederick, E., Manizade, S., Martin, C., Sonntag, J., Swift, R., Thomas, R., Wright, W., Yungel, J., 2002. Airborne laser altimetry mapping of the Greenland ice sheet: application to mass balance assessment. *Journal of Geodynamics*, 34(3), pp. 391-403.

Ahokas, E., Kaasalainen, S., Hyyppä, J., Suomalainen, J., 2006. Calibration of the Optech ALTM 3100 laser scanner intensity data using brightness targets. In: *The International Archives of the Photogrammetry, Remote Sensing and Spatial Information Sciences*, Marne-la-Vallée, France, Vol. XXXVI, Part A1, on CD-ROM.

Arnold, N.S., Rees, W.G., Devereux, B.J., Amable, G.S., 2006. Evaluating the potential of high-resolution airborne LiDAR data in glaciology. *International Journal of Remote Sensing*, 27(5-6), pp. 1233-1251.

Baltsavias, E.P., Favey, E., Bauder, A., Bösch, H., Pateraki, M., 2001. Digital Surface Modelling by Airborne Laser Scanning and Digital Photogrammertry for Glacier Monitoring. *Photogrammetric Record*, 17(98), pp. 243-273.

Bamber, J.L., Kwok, R., 2004. Remote sensing techniques for observing land and sea ice. In: *Mass balance of the cryosphere: observations and modelling of contemporary and future changes*. Cambridge University Press, pp. 59-113.

Da, T.K.F., 2006. 2D Alpha Shapes. In: *CGAL-3.2 User and Reference Manual (CGAL Editorial Board)*. http://www.cgal.org/Manual/3.2/doc_html/cgal_manual/contents.html (accessed 1 May 2007).

Edelsbrunner, H., Mücke, E.P., 1994. Three-dimensional alpha shapes. *ACM Transactions on Graphics*, 13(1), pp. 43-72.

Filin, S., Pfeifer, N., 2006. Segmentation of airborne laser scanning data using a slope adaptive neighborhood. *ISPRS Journal of Photogrammetry and Remote Sensing*, 60(2), pp. 71-80.

Geist, T., Lutz, E., Stötter, J., 2003. Airborne laser scanning technology and its potential for applications in glaciology. In: *The International Archives of the Photogrammetry, Remote Sensing and Spatial Information Sciences*, Dresden, Vol. XXXIV, Part 3/W13, pp. 101-106.

Höfle, B., Rutzinger, M., Geist, T., Stötter, J., 2006. Using airborne laser scanning data in urban data management - set up of a flexible information system with open source components. In*: Proceedings of UDMS 2006: 25th Urban Data Management Symposium*, Aalborg, Denmark, pp. 7.11-7.23.

Höfle, B., Pfeifer, N., 2007. Correction of laser scanning intensity data: data and model-driven approaches. *ISPRS Journal of Photogrammetry and Remote Sensing*, doi:10.1016/j.isprsjprs.2007.05.008 (in press).

Hook, S.J., 2007. ASTER Spectral Library. Jet Propulsion Laboratory, Californian Institute of Technology, http://speclib.jpl.nasa.gov/ (accessed 1 May 2007)

Hopkinson, C., Demuth, M.N., 2006. Using airborne lidar to assess the influence of glacier downwasting on water resources in the Canadian Rocky Mountains. *Canadian Journal of Remote Sensing*, 32 (2), pp. 212-222.

Jackson, M., Sharov, A.I., Geist, T., Elvehøy, H., Pellikka, P., 2001. OMEGA - User Requirement Document. Project Report, 16 p.

Kennett, M., Eiken, T., 1997. Airborne measurement of glacier surface elevation by scanning laser altimeter. *Annals of Glaciology*, 24, pp. 293-296.

Kodde, M.P., Pfeifer, N., Gorte, B.G.H., Geist, T., Höfle, B., 2007. Automatic glacier surface analysis from airborne laser scanning. In: *The International Archives of the Photogrammetry, Remote Sensing and Spatial Information Sciences*, this volume.

Lutz, E., Geist, T., Stötter, J., 2003. Investigations of airborne laser scanning signal intensity on glacial surfaces - Utilizing comprehensive laser geometry modeling and orthophoto surface modeling (a case study: Svartisheibreen, Norway). In: *The International Archives of the Photogrammetry, Remote Sensing and Spatial Information Sciences*, Dresden, Vol. XXXIV, Part 3/W13, pp. 143-148.

Rabbani, T., Heuvel, F.A. van den, Vosselman G., 2006. Segmentation of point clouds using smoothness constraint. In: *The International Archives of the Photogrammetry, Remote Sensing and Spatial Information Sciences*, Dresden, Vol. XXXVI, Part 5, pp. 248-253.

Rees, W.G., 2005. *Remote Sensing of Snow and Ice*. Taylor & Francis.

Wolfe, W.L., Zissis, G.J., 1993. *The Infrared Handbook*. Revised Edition. IRIA Series in Infrared and Electro Optics. The Infrared Information Analysis (IRIA) Center, Environmental Research Institute of Michigan.